



HAL
open science

Predictive control with efficiency optimization and normalization for a multilevel converter

Jean-Yves Gauthier, Xuefang Lin-Shi, Alexandru Avramoae

► **To cite this version:**

Jean-Yves Gauthier, Xuefang Lin-Shi, Alexandru Avramoae. Predictive control with efficiency optimization and normalization for a multilevel converter. 2013 IEEE SLED/PRECEDE, Oct 2013, Munich, Germany. s4p3, <10.1109/SLED-PRECEDE.2013.6684487>. <hal-00875809>

HAL Id: hal-00875809

<https://hal.science/hal-00875809v1>

Submitted on 19 Jun 2025

HAL is a multi-disciplinary open access archive for the deposit and dissemination of scientific research documents, whether they are published or not. The documents may come from teaching and research institutions in France or abroad, or from public or private research centers.

L'archive ouverte pluridisciplinaire **HAL**, est destinée au dépôt et à la diffusion de documents scientifiques de niveau recherche, publiés ou non, émanant des établissements d'enseignement et de recherche français ou étrangers, des laboratoires publics ou privés.



HAL Authorization

Predictive control with efficiency optimization and normalization for a multilevel converter

Jean-Yves Gauthier, Xuefang Lin-Shi, Alexandru Avramoae

Laboratoire Ampère, Université de Lyon, Institut National des Sciences Appliquées de Lyon
21 avenue Jean Capelle, 69621 Villeurbanne, France

Abstract—The good performances of model predictive control for power converters were demonstrated for multi-objective control. A relevant example is the multilevel flying capacitor electronic converter in which both capacitor voltages and output current have to be controlled. Moreover, the efficiency is an essential factor in electrical converter design but few papers focused on it in the control point of view. This paper presents a predictive control scheme for a multilevel converter which minimizes a cost function including a loss related term. The inclusion of a large number of elements into the cost function requires the tuning of many parameters. Normalization of the cost function is introduced in order to help the control designer to choose suitable parameters. Simulation and experimental tests prove that a trade-off between efficiency and accuracy can be achieved by controller adjustment.

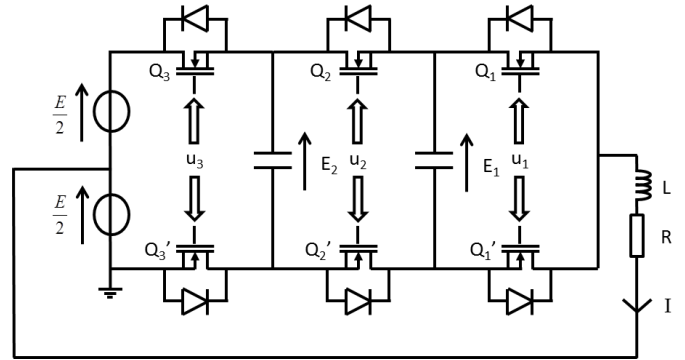


Fig. 1. Electrical scheme of the studied converter.

I. INTRODUCTION

Most control laws in power electronic converters focus on its static and dynamic performances. But few of them take directly into account the converter losses, which are generally reduced indirectly by limiting the switching frequency. For many converter architectures, the static and dynamic performances and the energy efficiency depend on this frequency. Thus it is interesting to include a criterion of energy efficiency in the control law, implying a trade-off between this efficiency and the control performance. In [1], a predictive control taking into account switching losses of a matrix converter is presented. A trade-off between control performance and converter efficiency must be made.

In this paper, a four-level three-cell converter is studied. The control objectives are not only to impose jointly the load current and the capacitor voltages, but also to reduce the switching losses. To accomplish these objectives, a model predictive control including switching loss criterion is applied. As real-time computation constraint is strong, a simplified switching loss model is designed. A generalized method for the normalization of the cost function will be proposed in order to have weight parameters focused in a certain range without unity. The normalization can be useful for control designers when many parameters have to be tuned. The control algorithm is presented and simulations show the effectiveness of this control method. Experimental set-up was also build and some results are discussed.

II. THE MULTILEVEL CONVERTER

A model of the flying capacitor converter depicted in figure 1 with ideal switches can be written as:

$$\dot{X} = A \cdot X + B \cdot E \quad X = \begin{pmatrix} E_1 \\ E_2 \\ I \end{pmatrix} \quad (1)$$

$$A = \begin{pmatrix} 0 & 0 & \frac{u_2 - u_1}{C_1} \\ 0 & 0 & \frac{u_3 - u_2}{C_2} \\ \frac{u_1 - u_2}{L} & \frac{u_2 - u_3}{L} & -\frac{R}{L} \end{pmatrix} \quad B = \begin{pmatrix} 0 \\ 0 \\ \frac{2 \cdot u_3 - 1}{2L} \end{pmatrix}$$

where E_1 , E_2 and I are respectively the voltage of the first (C_1) and second (C_2) flying capacitors and the current into the load. The load is composed of a serial resistor R and inductor L . The supplied voltage E is considered constant and is divided into two equal parts. The boolean control variables are u_1 , u_2 and u_3 . For $j = 1, 2, 3$, if $u_j = 0$, then the upper switch Q_j is open and the lower one Q'_j is closed. If $u_j = 1$, then the upper switch Q_j is closed and the lower one Q'_j is open.

For a flying capacitor multilevel converter, in addition to the output electrical current, the capacitor voltages should be maintained at constant values. Some solutions have been already proposed in [2], which don't take into account the converter efficiency.

As mentioned previously, we introduce a model for converter losses. These last can be approximated by switching and conduction losses. As the load current I always flows only through three switches, it is difficult to act on conduction losses by changing the control laws. So we focus only on

the switching losses. The following equation describes the lost energy after a switching sequence in one switch.

$$\mathcal{E}^{lost} = \int_{t_b}^{t_a} I^{sw}(t) \cdot V^{sw}(t) dt \quad (2)$$

where t_b , t_a , $I^{sw}(t)$, $V^{sw}(t)$ are respectively the times before and after a switching sequence, the current through the switch and the voltage on the switch.

In order to reduce the computation time in real-time, a simplified model for loss modeling was used. The lost energy after a switching sequence in one switch becomes:

$$\mathcal{E}^{ON \rightarrow OFF} = \Psi \cdot |I^{sw}(t_b) \cdot V^{sw}(t_a)| \quad (3)$$

$$\mathcal{E}^{OFF \rightarrow ON} = \Psi \cdot |I^{sw}(t_a) \cdot V^{sw}(t_b)| \quad (4)$$

Ψ is a parameter related to the time duration and the shape of the switching sequence. Two examples of switching sequences are presented on figure 2, where t_{sw} is the switching duration. The relation between Ψ and t_{sw} can be calculated : in the first example, $\Psi = \frac{t_{sw}}{6}$ and in the second one, $\Psi = \frac{t_{sw}}{2}$.

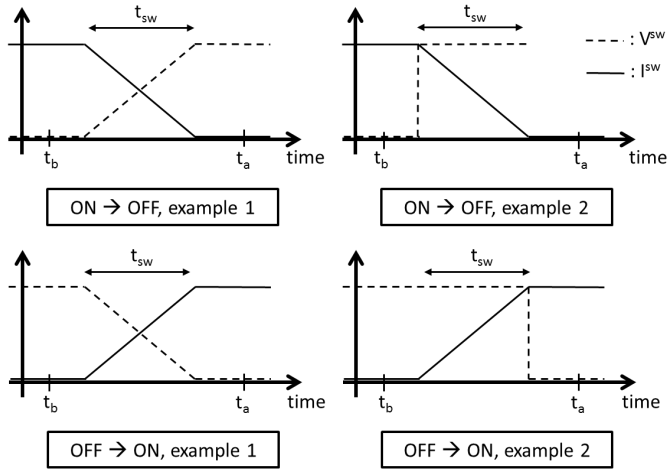


Fig. 2. Current and voltage during a switching sequence. Two examples are chosen (left and right figures with on top the ON to OFF and on bottom the OFF to ON sequences).

III. MODEL PREDICTIVE CONTROL

An overview of model predictive control applied to power electronic converters can be found in [3] and in [4]. For each switching configuration, a prediction of the future state is done and a cost function is calculated. The switching configuration corresponding to the best cost function is then applied for next sample time.

A. Predictive control applied to multilevel converter

In this converter, the three boolean control variables give eight configurations ($i = 1, \dots, 8$). A diagram of the basic predictive control is shown in figure 3(a). The outputs of the predictive model are the eight predicted state vectors of the converter for next sample instant. For each sample time T and configuration, the future state \hat{X}_i^{k+1} is calculated in real-time:

$$\hat{X}_i^{k+1} = X^k + (A_i \cdot X^k + B_i \cdot E) \cdot T \quad (5)$$

Each predicted vector \hat{X}_i^{k+1} is used to evaluate a corresponding cost function CF_i that weights different control objectives. At last, the controller chooses the switching state of the predicted vector i that gives the best cost function. A cost function, that takes into account the capacitor voltage error and current error is used in [5].

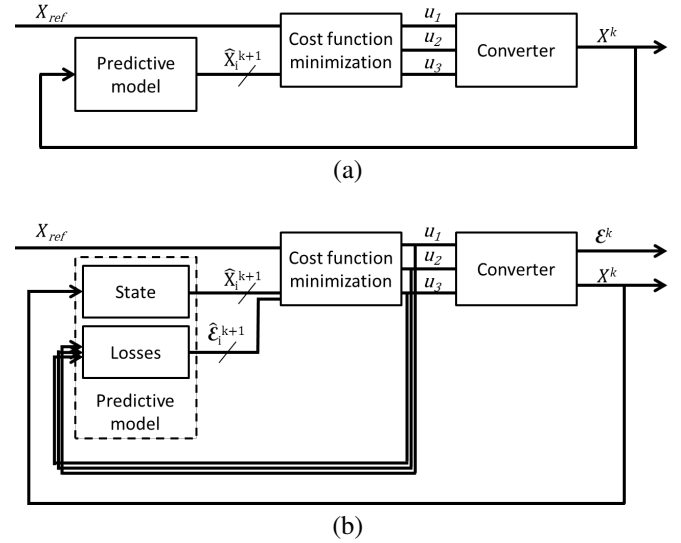


Fig. 3. Predictive control scheme without (a) and with (b) switching loss prediction.

B. Predictive control with efficiency optimization

In order to add efficiency optimization in the control law, a term depending on the switching frequency can be included in the cost function [6]. An alternative method, used here, is the integration of a loss related term in the cost function [1]. A general diagram of the proposed improved predictive control including loss prediction is shown in figure 3(b). A prediction of the losses is added in the cost function.

By considering that the switching sequence is very short in comparison to the period T and that it will start immediately after the calculation, all the switching sequences are considered at time $t = k \cdot T$. The predicted loss for the switch Q_1 (see figure 1) is thus calculated by using the equations (3) and (4):

$$\hat{\mathcal{E}}_{Q_1}^{k+1}(ON \rightarrow OFF) = \hat{\mathcal{E}}_{Q_1}^{k+1}(OFF \rightarrow ON) = \Psi \cdot |I^k \cdot E_1^k| \quad (6)$$

This loss appears only if the future control \hat{u}_{1i}^{k+1} is different than the actual control u_1^k , the final expression for the predicted loss concerning the switch Q_1 becomes thus:

$$\hat{\mathcal{E}}_{Q_1}^{k+1} = \Psi \cdot |I^k \cdot E_1^k| \cdot (\hat{u}_{1i}^{k+1} \oplus u_1^k) \quad (7)$$

where \oplus is the exclusive OR logical operator.

The total predicted loss $\hat{\mathcal{E}}_i^{k+1}$ for each configuration is obtained by adding the lost of each switch, calculated with the same approach as for Q_1 .

$$\hat{\mathcal{E}}_i^{k+1} = 2 \cdot \Psi \cdot |I^k| \cdot \left[|E_1^k| \cdot (\hat{u}_{1i}^{k+1} \oplus u_1^k) + |E_2^k - E_1^k| \cdot (\hat{u}_{2i}^{k+1} \oplus u_2^k) + |E - E_2^k| \cdot (\hat{u}_{3i}^{k+1} \oplus u_3^k) \right] \quad (8)$$

C. Cost function choice

The control objectives are given as follow:

- tracking the load current reference I_{ref} (In our example, I_{ref} was chosen equal to a sine wave, therefore the converter acts as an inverter);
- keeping the voltage of the two capacitors constant ($E_1 = E_{1ref} = E/3$ and $E_2 = E_{2ref} = 2 \cdot E/3$) in order to balance the voltages seen by each transistor;
- improving the energy efficiency.

These objectives may be balanced in the following cost function:

$$CF_i^2 = K_0 \left[\left(E_{1ref} - \widehat{E}_{1i}^{k+1} \right)^2 + \left(E_{2ref} - \widehat{E}_{2i}^{k+1} \right)^2 \right] + K_1 \left(I_{ref} - \widehat{I}_i^{k+1} \right)^2 + K_2 \left(\widehat{\mathcal{E}}_i^{k+1} \right)^2 \quad (9)$$

The first parameter K_0 of the cost function weights the capacitor voltage errors, the second one K_1 the load current error and the third one K_2 the converter switching losses. To balance each term, only the ratios $\frac{K_1}{K_0}$ and $\frac{K_2}{K_0}$ are required. If we want to decrease the capacitor voltage errors, we only need to decrease both K_1 and K_2 by holding K_0 constant.

D. Normalization of the cost function

A difficulty of the model predictive control is the choice of the weighting parameters. We propose a generalized method to make this task easier. Units of K_0 , K_1 and K_2 are different, so it is difficult to define the range of each weight. We propose to add normalization terms into the cost function as follow:

$$(CF_i')^2 = \left(\frac{E_{1ref} - \widehat{E}_{1i}^{k+1}}{\Delta E_1} \right)^2 + \left(\frac{E_{2ref} - \widehat{E}_{2i}^{k+1}}{\Delta E_2} \right)^2 + K_1' \left(\frac{I_{ref} - \widehat{I}_i^{k+1}}{\Delta I} \right)^2 + K_2' \left(\frac{\widehat{\mathcal{E}}_i^{k+1}}{\Delta \mathcal{E}} \right)^2 \quad (10)$$

K_1' and K_2' are the new weighting parameters. To calculate the normalization terms ΔE_1 , ΔE_2 , ΔI and $\Delta \mathcal{E}$, an approach with the difference between maximum and minimum variations during one sample time is used.

The detail of the method is developed for ΔE_1 . The first line of the equation (5) gives:

$$\widehat{E}_{1i}^{k+1} = E_1^k + \left(\frac{u_2 - u_1}{C_1} \cdot I^k \right) \cdot T \quad (11)$$

By writing this equation for the eight predictions, the maximum and minimum values can be calculated:

$$\left(\widehat{E}_{1i}^{k+1} \right)_{MAX} = E_1^k + \left(\frac{1}{C_1} \cdot I^k \right) \cdot T \quad (12)$$

$$\left(\widehat{E}_{1i}^{k+1} \right)_{MIN} = E_1^k + \left(\frac{-1}{C_1} \cdot I^k \right) \cdot T \quad (13)$$

The normalization term is then defined as the difference between the maximum and minimum values:

$$\Delta E_1 = \left(\widehat{E}_{1i}^{k+1} \right)_{MAX} - \left(\widehat{E}_{1i}^{k+1} \right)_{MIN} = \frac{2 \cdot I^k \cdot T}{C_1} \quad (14)$$

Following this method for other variables, the normalization terms are calculated as:

$$\Delta E_1 = \frac{2 \cdot I^k \cdot T}{C_1} \quad \Delta E_2 = \frac{2 \cdot I^k \cdot T}{C_2} \quad (15)$$

$$\Delta I = \frac{E \cdot T}{L} \quad \Delta \mathcal{E} = 2 \cdot \psi \cdot E \cdot I^k \quad (16)$$

We can notice that, except for ΔI , the normalization terms are not constant but depend on the measured current I^k .

IV. SIMULATION RESULTS

During the following, the load current reference will be a sine wave of 4 A peak to peak and 50 Hz. Moreover, $E = 200$ V, $L = 50$ mH, $R = 33$ Ω , $C_1 = C_2 = 33$ μ F, $\psi = 0.5$ μ s, $T = 70$ μ s. Simulations are made with the help of the Matlab / Simulink software. Bogacki-Shampine integration solver was used. The simulation sample time was chosen equal to 1 μ s and the stop time equal to 0.2 s. The converter is modeled by the equation (1). Equations (3) and (4) are used to estimate the total switching loss energy. The dissipated power is obtained by dividing the lost energy by the total simulation time.

A. High accuracy for capacitor voltages

For the first simulation (figure 4 (a)), the values $K_1' = 0$ and $K_2' = 0.1$ are chosen so small that the main goal corresponds to maintain constant capacitor voltages. To reach this objective, the switching configuration which actuates simultaneously the three control variables ($u_1 = u_2 = u_3$) is selected. As the resistors of the two capacitors are neglected, its voltages do not change and errors on E_1 and E_2 are equal to zero. The choice between $u_1 = u_2 = u_3 = 0$ or $u_1 = u_2 = u_3 = 1$ is made by judging the current error. The switching losses power was estimated to 0.93 W.

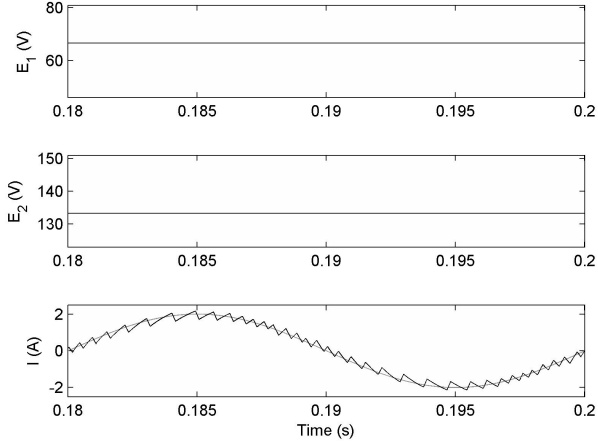
For the second simulation (figure 4 (b)), $K_1' = 0$ and $K_2' = 0.3$. These two values are still small, the main goal always is to maintain constant capacitor voltages. The controller actuates simultaneously the three control variables ($u_1 = u_2 = u_3$). As K_2' is different to 0, the energy loss criterion takes part in the cost function. It leads to reduce the switching frequency as shown in figure 4 (b). The dissipation due to switching sequences decreases significantly (0.33 W).

B. Trade-off between current error, voltage errors and losses

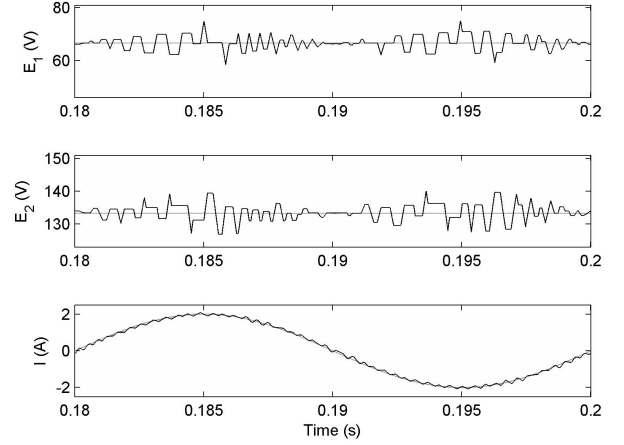
In order to focus on current accuracy, the value of K_1' is significantly increased ($K_1' = 20$). This leads to an increase in the capacitor voltage errors.

First, a simulation is made without energy loss optimization ($K_2' = 0$ and $K_1' = 20$). As shown in figure 5(a), the current error is smaller than the one of figure 4 (a), but the capacitor voltage accuracy is degraded. The switching loss power for the converter was estimated to about 0.89 W.

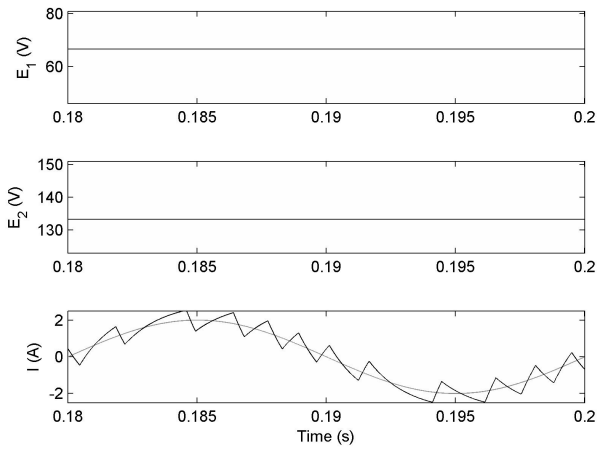
Secondly, by choosing $K_2' = 15$, the energy loss criterion has been taken into account and the electrical current and capacitor voltages was less accurate than the previous simulation (see figure 5(b)). Consequently the switching loss power was divided by more than two (about 0.42 W). We can remark that the controller automatically decreased the switching frequency and improved the efficiency.



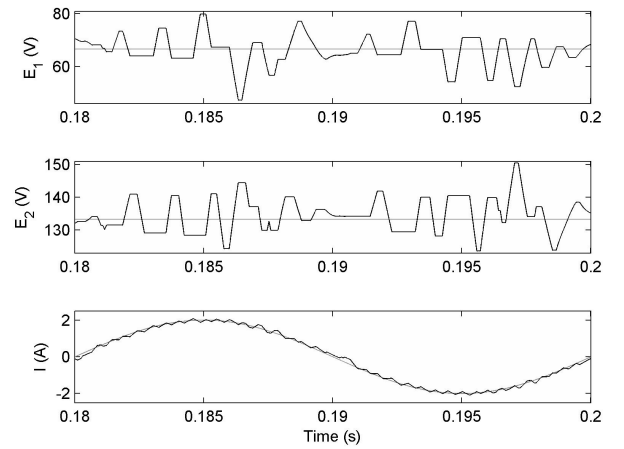
(a)



(a)



(b)



(b)

Fig. 4. Simulation results (a) without ($K_2' = 0$ and $K_1' = 0.1$) and (b) with energy loss optimization ($K_2' = 0.3$ and $K_1' = 0.1$). Black lines correspond to actual values of capacitor voltages and load current, light grey ones are reference values.

C. Normalization effect

In the last simulation, $K_2' = 15$ and $K_1' = 20$ were used in the controller. Without normalization, equivalent values for control parameters are: $K_0 = 1$, $K_1 = 1.8 \cdot 10^4 \text{ V}^2 \cdot \text{A}^{-2}$ and $K_2 = 6.7 \cdot 10^9 \text{ V}^2 \cdot \text{J}^{-2}$. The difficulty of studying the influence of unnormalized parameters is then clearly to be seen. Another advantage of the normalization is to make graphic analysis easier. By changing K_1' and K_2' parameters, it is possible to create three dimensional plots for the switching loss power, the capacitor voltage errors and the load current error (see figure 6). An increase of K_2' parameter induces a decrease of switching losses, but errors on capacitor voltages and current increase. By increasing K_1' parameter, a decrease of the load current error is observed but a small increase of voltage errors and switching loss appears.

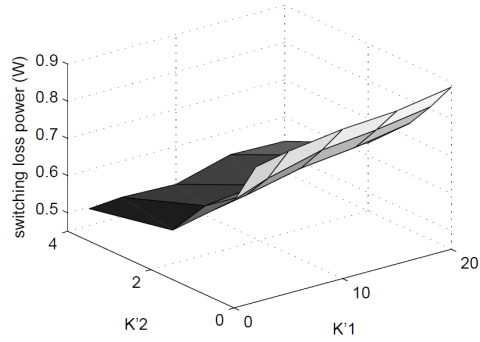
As underlined in the subsection III-D, the normalization

Fig. 5. Simulation results (a) without ($K_2' = 0$ and $K_1' = 20$) and (b) with energy loss optimization ($K_2' = 15$ and $K_1' = 20$). Black lines correspond to actual values of capacitor voltages and load current, light grey ones are reference values.

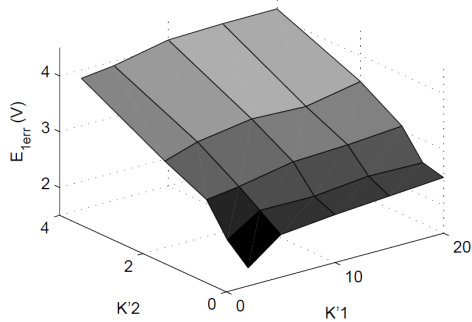
terms are depending on the measured current I_k . As the current reference is a sine wave, the value of these terms strongly changes during the sine wave period. In figure 7, a comparison is made between simulations with the relations described by equations (15)(figure 7 (a)) and the same ones but with constant I_k of 2 A in order to have constant normalization terms. In this last case (see figure 7 (b)), the current error is smaller when the current reference is near zero (at time 0.18, 0.19 and 0.2) but the error on capacitor voltages increase at these instants.

V. EXPERIMENTAL TEST-BENCH

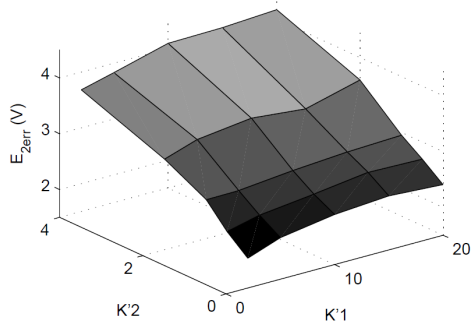
The experimental test-bench is shown in figure 8. The converter is manufactured with 6 IRF740 MOSFET. It is supplied by 2 Xantrex voltage sources with capacitors. The component values are the same as that for the simulation. The drivers for the transistors are controlled by optical fibers



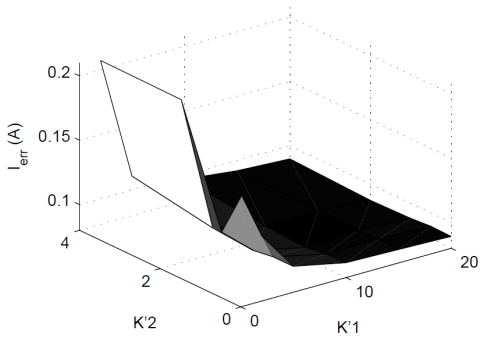
(a)



(b)

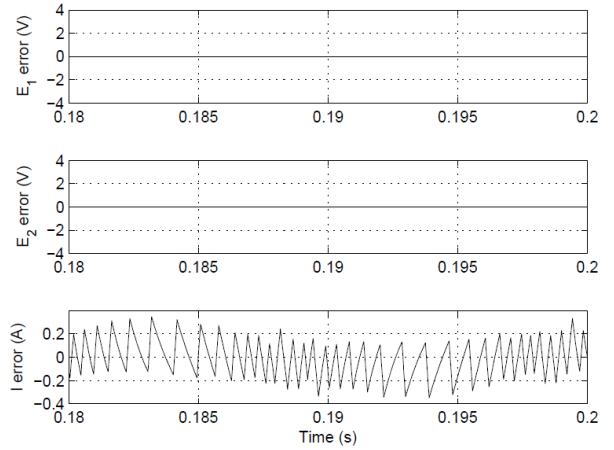


(c)

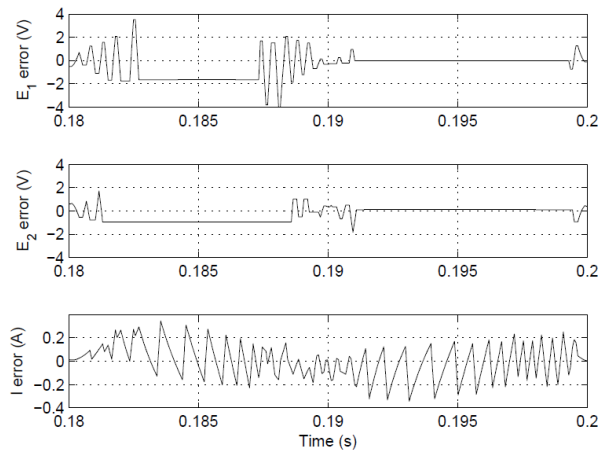


(d)

Fig. 6. Simulations results. Switching loss power, errors on capacitor voltages and error on load current versus cost function weights K'_1 and K'_2 .



(a)



(b)

Fig. 7. Comparison between normalization described by equations (15) (a) and normalization with constant terms (b). The parameters of the controller are $K'_2 = 0$ and $K'_1 = 0.1$.

coming from a FPGA that ensures a non-optimized dead-time of $6 \mu\text{s}$. The inputs of the FPGA board were connected to three digital outputs of a DS1104 dSPACE board. Measurements of the two capacitor voltages and the load current are made by using probes. Moreover, a thermal probe was used in order to have an image of the real power consumption of the converter.

Some results are presented in figure 9. A normalization depending on the measured current terms was used. Ambient temperature was of about 25°C during all experiments. A first test performed without loss optimization ($K'_2 = 0$) is used as a reference and the temperature was measured at 42.6°C for $T=70 \mu\text{s}$ and $K'_1 = 11$ (figure 9, first test). If we want to decrease switching losses, an increase of sample period T could be used ($T=280 \mu\text{s}$) but current error increases dramatically (figure 9, second test). By adjusting K'_1 parameter, current error could decrease but an huge increase of capacitor voltage errors appears (figure 9, third test).

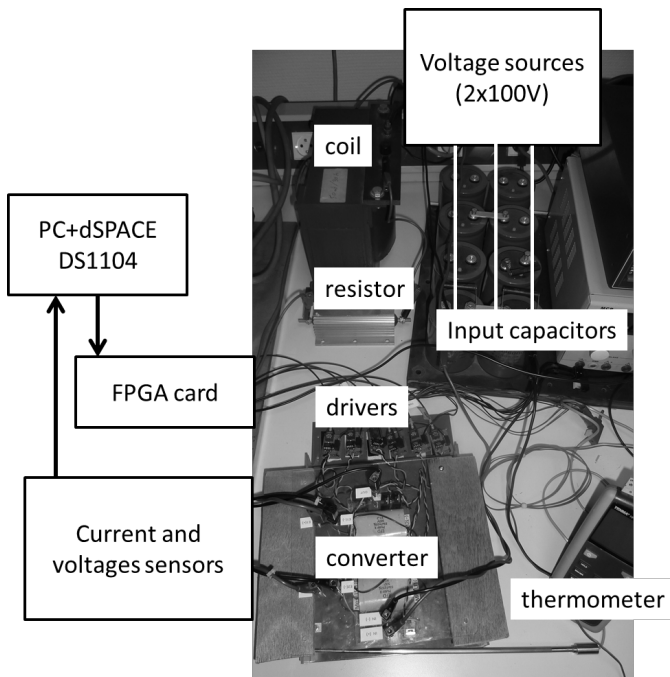


Fig. 8. Experimental test-bench.

An alternative way to decrease power consumption is to introduce the loss optimization ($K'_2 \neq 0$) in the controller. The weighting parameters of the last test of the figure 9 were chosen as $K'_2 = 4$ and $K'_1 = 11$. Comparing to the second and third controllers, smaller sample time is used ($T=70 \mu s$) with same losses. That way, a smaller current error can be achieved with reasonable voltage errors.

These tests show that the direct consideration of the losses into a controller achieves better results than an indirect consideration only by choosing a larger sample time period. However, this kind of control needs a higher computing frequency than the effective switching frequency and it could be a drawback for high frequency converters. The value $T=70 \mu s$ is limited by the control board used in this paper.

VI. CONCLUSION

In this paper, we applied model predictive control to a multilevel converter including a consideration on the efficiency of the global converter. A normalization of the cost function was proposed in order to help the control designer to tune the parameters. Two ways for normalization were studied in simulation, the direct one depending on the measured current can be used for large current value conditions, and the extended one having constant weights. Influences of each control parameters were studied in simulation and experimentation. A trade-off between control performance and power consumption can easily be made. The method is well adaptable to other converters.

REFERENCES

- [1] R. Vargas, U. Ammann, and J. Rodriguez, "Predictive approach to increase efficiency and reduce switching losses on matrix converters," *Power Electronics, IEEE Transactions on*, vol. 24, no. 4, pp. 894–902, 2009.

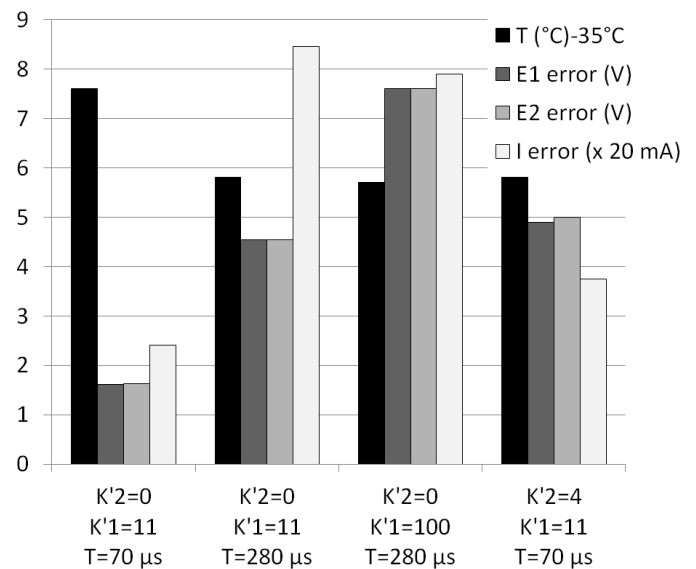


Fig. 9. Experimental comparisons between different control laws.

- [2] D. Patino, R. P. Bâja, M., H. Cormerais, J. Buisson, and C. Iung, "Alternative control methods for dc-dc converters: An application to a four-level three-cell dc-dc converter," *Int. J. Robust Nonlinear Control*, vol. 21, pp. 1112–1133, 2011.
- [3] J. Rodriguez and P. Cortes, *Predictive Control of Power Converters and Electrical Drives*. John Wiley & Sons, Ltd, 2012.
- [4] A. Ziani, A. Llor, and M. Fadel, "Model predictive current controller for four-leg converters under unbalanced conditions," in *Power Electronics and Applications (EPE 2011), Proceedings of the 2011-14th European Conference on*, 2011, pp. 1–10.
- [5] M. Trabelsi, J. Retif, X. Lin-Shi, X. Brun, F. Morel, and P. Bevilacqua, "Hybrid control of a three-cell converter associated to an inductive load," in *IEEE Power Electronics Specialists Conference, 2008. PESC 2008.*, 15-19 June 2008, pp. 3519–3525.
- [6] R. Vargas, P. Cortés, U. Ammann, J. Rodriguez, and J. Pontt, "Predictive control of a three-phase neutral-point-clamped inverter," *IEEE TRANSACTIONS ON INDUSTRIAL ELECTRONICS*, vol. 54, no. 5, pp. 2697–2705, 2007.